I&EC research
Industrial & Engineering Chemistry Research

Article

pubs.acs.org/IECR

Distributed Extended Kalman Filtering for Wastewater Treatment Processes

Jing Zeng,[‡,¶] Jinfeng Liu,[*,¶] Tao Zou,[§] and Decheng Yuan[‡]

[‡]Liaoning Province Key Laboratory of Control Technology for Chemical Processes, Shenyang University of Chemical Technology, Shenyang 110142, China

[¶]Department of Chemical & Materials Engineering, University of Alberta, Edmonton, Alberta T6G 2V4, Canada

[§]Shenyang Institute of Automation, Chinese Academy of Sciences, Shenyang 110016, China

ABSTRACT: A wastewater treatment plant is a large-scale nonlinear system including a series of biological reactors and a settler. In this work, we propose a distributed state estimation scheme for wastewater treatment processes in the context of extended Kalman filtering. Specifically, we consider a wastewater treatment process that includes a five-compartment reactor and an ideal splitter. First, we present a method to design the sensor network for the process and then discuss how the process may be decomposed into subsystems for distributed state estimation. We present a detailed design of the distributed filters and a detailed distributed state estimation algorithm to coordinate the actions of the different filters. Without loss of generality, we consider the entire system as being decomposed into two subsystems. The proposed approach can be extended in a straightforward fashion to include more subsystems. The distributed scheme is compared with the corresponding centralized extended Kalman filtering scheme under different weather conditions. Simulation results show that the distributed scheme can give comparable estimation performance to the centralized scheme or even better performance than the centralized scheme. Also, the distributed estimation scheme is shown to have more stable performance under different noise conditions.

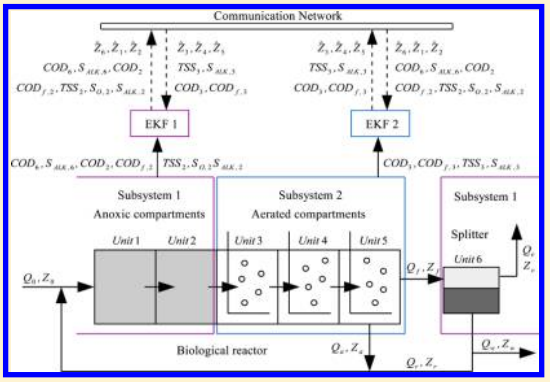

INTRODUCTION

Wastewater treatment is an important step in water recycling, and it involves complex biological and physical phenomena. A wastewater treatment plant (WWTP) is typically a large-scale nonlinear system including a series of biological reactors and a settler. The effluent quality of a wastewater treatment plant is closely related to the sustainability of the environment and normally is regulated by environmental legislations. The significant variability of the influent flow and the composition of the flow to a WWTP poses significant challenges in the associated control system design.

Different process control schemes have been reported for WWTPs. Proportional−integral (PI) control is one of the most commonly used strategies[1,2] because of its simplicity in design and implementation. Feedforward control has also been implemented together with PI control to improve the control performance.[3] While PI control can achieve the stability requirement in the operation, it cannot handle constraints and is not optimal. Model predictive control (MPC) is an online optimization-based approach and can take input and state constraints explicitly into account.[4] MPC as an optimal control method has also been widely used in the control of WWTPs.[5−9] The effectiveness of MPC was demonstrated in ref 5 with the application to a WWTP in Lancaster, England. In ref 6, a MPC tuning procedure was developed, and a nonlinear multiobjective MPC method was presented in ref 7. Different hierarchical control structures for WWTPs were discussed in ref 8. In ref 10, an economic MPC algorithm was applied to a WWTP, and the economic MPC performance was compared with PI and regular MPC. It was shown that economic MPC is able to achieve improved effluent quality.

While there are many results on the control system design for WWTPs, relatively less attention has been given to the state estimation of WWTPs. State estimation is a process of constructing system states based on output measurements and a system model. State estimation is closely related to the control and monitoring of WWTPs and is an important topic in the operation of WWTPs because many relevant states in wastewater treatment are not measurable or are subject to significant noise. Two commonly used state estimation methods for nonlinear systems are the extended Kalman filter (EKF)[11] and the moving horizon state estimation (MHE).[12] To handle nonlinearity, in EKF, successive linearization of the nonlinear system is performed every sampling time. The MHE is an optimization-based state estimator that can handle nonlinear systems and system constraints. However, MHE is usually very computationally demanding, especially for nonlinear systems.

Received: February 5, 2016
Revised: April 26, 2016
Accepted: June 23, 2016
Published: June 23, 2016

DOI: 10.1021/acs.iecr.6b00529
Ind. Eng. Chem. Res. 2016, 55, 7720−7729

In ref 13, both EKF and MHE were applied to the state estimation of a WWTP. It was shown that both the EKF and the MHE can give good estimation performance even under difficult conditions. Because the EKF and MHE give similar performance, EKF was recommended because of its simplicity and efficiency in implementation. In ref 13, the EKF was implemented in a centralized framework. For large-scale systems, centralized implementation is not favorable from fault-tolerance as well as organizational points of view.[14]

Motivated by the above consideration, in this work, we propose a distributed state estimation scheme for WWTPs in the context of EKF. The main contributions of this work include (1) a detailed subsystem decomposition approach for the WWTP system, (2) a detailed design of distributed extended Kalman filter and an algorithm to coordinate the actions of the different filters, and (3) the application of the distributed EKF to the WWTP compared with the centralized scheme under different weather conditions. The proposed distributed state estimation provides an alternative scheme to the centralized estimation scheme and is inspired by our previous work on distributed MHE.[15,16] Specifically, in this work, we consider a typical wastewater treatment process that includes a five-compartment reactor and an ideal splitter. First, we propose a method for sensor network design and subsystem decomposition for distributed state estimation; then we present the detailed design of the distributed EKFs. A detailed distributed state estimation algorithm is also introduced to coordinate the actions of the different EKFs. Without loss of generality, we consider the entire system as decomposed into two subsystems. The proposed approach can be extended in a straightforward fashion to include more subsystems. The distributed EKF scheme is compared with the corresponding centralized EKF under different weather conditions.

WASTEWATER TREATMENT PROCESSES

The Benchmark Simulation Model No. 1 (BSM1) is composed of a five-compartment activated sludge reactor and a secondary settler, which is a popular benchmark for evaluating different control strategies for WWTP. In this work, the process model is based on BSM1 benchmark, and the plant layout is shown in Figure 1.[13,17] The five sludge reactors in BSM1 remain unchanged while the secondary settler is replaced by a membrane filtration unit, which is modeled as an ideal splitter.[13] The activated sludge reactor section includes two anoxic compartments (anoxic section) and three aerobic compartments (aerated section). In this process, two elementary reactions take place in the two different sections: (1) Denitrification biological reactions take place in the anoxic section where bacteria change nitrate into nitrogen. (2) Nitrification reactions in which the bacteria oxidize ammonium to nitrate take place in the aerated section. Wastewater is feed into the first anoxic reactor at flow rate Q_0 and concentration Z_0. [A generic compound Z is used in the description to denote the different compounds (see Table 2) in the wastewater treatment plant to simplify the description.] A portion of the effluent of the last aerated reactor is recycled back to the first anoxic reactor at flow rate Q_a and concentration Z_a (i.e., internal recycle), and the rest of the effluent is fed into the splitter at flow rate Q_f and concentration Z_f. The processed water leaves from the top of the splitter at flow rate Q_e and concentration Z_e. The generated sludge is withdrawn from the bottom of the splitter at flow rate Q_w and concentration Z_w. A second recycle stream from the splitter is fed back to the first anoxic reactor at flow rate Q_r and concentration Z_r (i.e., external recycle).

The biological phenomena taking place in the five biological compartments are described by the Activated Sludge Model No. 1 (ASM1).[17] In the simulation model, eight biological processes are used to describe the biological behavior, as in Table 1. In these processes, 13 different compounds are considered, and the concentrations of these compounds are the state variables of the simulation model. The definitions of these state variables are given in Table 2. A total of 78 ordinary

Table 1. List of Biological Processes

1	aerobic growth of heterotrophs
2	anoxic growth of heterotrophs
3	aerobic growth of autotrophs
4	decay of heterotrophs
5	decay of autotrophs
6	ammonification of soluble organic nitrogen
7	hydrolysis of entrapped organics
8	hydrolysis of entrapped organic nitrogen

Table 2. List of State Variables

notation	definition	unit
S_I	soluble inert organic matter	g COD/m^3
S_S	readily biodegradable substrate	g COD/m^3
X_I	particulate inert organic matter	g COD/m^3
X_S	slowly biodegradable substrate	g COD/m^3
$X_{B,H}$	active heterotrophic biomass	g COD/m^3
$X_{B,A}$	active autotrophic biomass	g COD/m^3
X_P	particulate products arising from biomass decay	g COD/m^3
S_O	oxygen	g (−COD)/m^3
S_{NO}	nitrate and nitrite nitrogen	g N/m^3
S_{NH}	NH_4^+ and NH_3 nitrogen	g N/m^3
S_{ND}	soluble biodegradable organic nitrogen	g N/m^3
X_{ND}	particulate biodegradable organic nitrogen	g N/m^3
S_{ALK}	alkalinity	mol/m^3

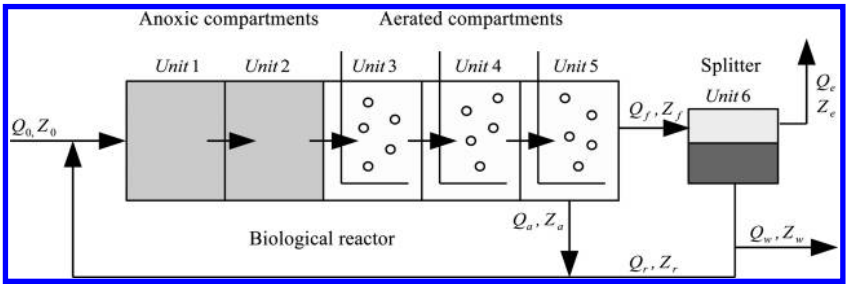

Figure 1. General overview of the modified BSM1.

DOI: 10.1021/acs.iecr.6b00529
Ind. Eng. Chem. Res. 2016, 55, 7720−7729

differential equations are used to described the dynamics of the entire plant in which each biological reactor and the splitter are described by 13 ordinary differential equations according to the 13 state variables.

In the model, the general equations of biological reactor (i.e., two anoxic reactors and three aerated reactors) on mass balances provided below.[17]

For $k = 1$ (reactor 1):

$$\frac{dZ_1}{dt} = \frac{1}{V_1}(Q_a Z_a + Q_r Z_r + Q_0 Z_0 + r_1 V_1 - Q_1 Z_1) \tag{1a}$$

$$Q_1 = Q_a + Q_r + Q_0 \tag{1b}$$

For $k = 2-5$ (reactor 2 to 5):

$$\frac{dZ_k}{dt} = \frac{1}{V_k}(Q_{k-1} Z_{k-1} + r_k V_k - Q_k Z_k) \tag{2a}$$

$$Q_k = Q_{k-1} \tag{2b}$$

Special case for oxygen ($S_{O,k}$)

$$\frac{dS_{O,k}}{dt} = \frac{1}{V_k}(Q_{k-1} S_{O,k-1} + r_k V_k + (K_L a)_k V_k (S_O^* - S_{O,k}) - Q_k S_{O,k}) \tag{3}$$

where the saturation concentration for oxygen is $S_O^* = 8\ g \cdot m^{-3}$ and r_k denotes the observed conversion rates of different compounds in reactor k; the detailed calculation of r_k can be found in ref 17.

As for the splitter, assuming there is no biological activity in it, the equations of mass balances can be described as follows:

For $k = 6$ (splitter):

Soluble compounds (i.e., S_I, S_S, S_O, S_{NO}, S_{NH}, S_{ND}, and S_{ALK}):

$$\frac{dZ_k}{dt} = \frac{1}{V_k}(Q_f Z_{k-1} + (Q_e + Q_r + Q_w) Z_k) \tag{4}$$

Note that for the well-mixed soluble compounds in the splitter, the concentrations of Z_e, Z_r, and Z_w for every soluble compound (S_I, S_S, S_O, S_{NO}, S_{NH}, S_{ND}, and S_{ALK}) are all the same and can be indicated as Z_k ($k = 6$). Moreover, the concentrations of the seven soluble compounds in the last aerated reactor are equal to the corresponding concentrations in the splitter, which means $Z_{k-1} = Z_k$ ($k = 6$) in eq 4.

Solid compounds (i.e., X_I, X_S, $X_{B,H}$, $X_{B,A}$, X_P, and X_{ND}):

$$\frac{dZ_k}{dt} = \frac{1}{V_k}(Q_f Z_{k-1} + (Q_r + Q_w) Z_k) \tag{5}$$

In the ideal splitter, we suppose that all six solid compounds precipitate in the bottom of the basin, so the concentration Z_e at the top of the splitter for the solid compounds are all zeros. The concentrations Z_r and Z_w are the same and can be described as Z_k ($k = 6$).

The flow rates of the plant layout in Figure 1 satisfy the following equations:

$$\begin{aligned} &Q_1 = Q_2 = Q_3 = Q_4 = Q_5 \\ &Q_1 = Q_a + Q_r + Q_0 \\ &Q_f = Q_5 - Q_a = Q_e + Q_r + Q_w = Q_e + Q_u \\ &Q_0 = Q_e + Q_w \end{aligned} \tag{6}$$

The above model of the WWTP can be described in a compact form as

$$\dot{x}(t) = f(x(t), u(t), w(t)) \tag{7a}$$

$$y(t) = Cx(t) + v(t) \tag{7b}$$

where $x \in \mathbb{R}^{78}$ is the vector of process state variables; w denotes random process noise/disturbances not explicitly described by the model; u denotes the manipulated input vector; y is the measured output vector; and v is a measurement noise vector. In this work, we consider distributed state estimation of the WWTP. Specifically, we propose a systematic approach for the design of distributed extended Kalman filters (EKF) for the WWTP. We will divide the entire WWTP into two subsystems, and for each subsystem, a local EKF is designed. The two EKFs communicate with each other and collaboratively estimate the entire states of the WWTP. We note that the proposed systematic design approach can be applied to design a distributed state estimation scheme with more subsystems.

SUBSYSTEM CONFIGURATION

In this section, the WWTP system will be decomposed into two subsystems for the purpose of distributed state estimation. In subsystem decomposition, the primary factor considered is the observability of the subsystem and the entire system. In addition to the observability consideration, we follow the following guidelines: (a) subsystem decomposition aligns with the system's physical topology is more favorable and (b) an operating unit in the WWTP is preferred to be associated with only one local estimator.

Available Measurements. In the WWTP, there are in total 48 states that can be measured using commercially available instruments.[13] For each of the five biological reactors and the ideal splitter, eight state variables or state related variables can be measured. They are (1) concentration of oxygen, S_O; (2) concentration of alkalinity, S_{ALK}; (3) concentration of ammonia, S_{NH}; (4) concentration of nitrate, S_{NO}; (5) chemical oxygen demand, COD; (6) filtered chemical oxygen demand, COD_f; (7) biological oxygen demand, BOD; and (8) total suspended solids, TSS. The definitions and expressions of these available measurements are given in Table 3.[13]

Table 3. List of Measured Outputs

notation	definition	expression
S_O	oxygen	S_O
S_{ALK}	alkalinity	S_{ALK}
S_{NH}	NH_4^+ and NH_3 nitrogen	S_{NH}
S_{NO}	nitrate and nitrite nitrogen	S_{NO}
COD	chemical oxygen demand	$S_I + S_S + X_S + X_I + X_{B,H} + X_{B,A}$
COD_f	filtered chemical oxygen demand	$S_I + S_S$
BOD	biological oxygen demand	$S_S + X_S$
TSS	total suspended solids	$X_I + X_S + X_{B,H} + X_{B,A} + X_P + X_{ND}$

Sensor Network Design and Subsystem Decomposition. In the wastewater treatment plant, to design a state estimation system, a prerequisite is that the entire plant and the two subsystems are observable. A system is said to be observable if, for a time interval $[t_0, t_1]$, given the input and output measurements over the interval it is possible to solve for the initial state $x(t_0)$.[18] The WWTP is a nonlinear process.

DOI: 10.1021/acs.iecr.6b00529
Ind. Eng. Chem. Res. 2016, 55, 7720−7729

In order to check its observability, we linearize the nonlinear model at different points along typical state trajectories and check the observability of these linearized models. This approximation approach was also used in ref 13. The linear approximation of the process at $x(t)$ can be described as the following form (assuming zero process and measurement noise without loss of generality):

$$\dot{x}(t) = A(t)x(t) + B(t)u(t)$$
$$y(t) = C(t)x(t) \tag{8}$$

where $A(t)$ and $C(t)$ are obtained by taking the Jacobian of eqs 7a and 7b at $x(t)$, respectively, as follows:

$$A(t) = \begin{bmatrix} \frac{\partial f_1}{\partial x_1} & \cdots & \frac{\partial f_1}{\partial x_n} \\ \vdots & \ddots & \vdots \\ \frac{\partial f_n}{\partial x_1} & \cdots & \frac{\partial f_n}{\partial x_n} \end{bmatrix}_{x=x(t)}, \quad C(t) = \begin{bmatrix} \frac{\partial y_1}{\partial x_1} & \cdots & \frac{\partial y_1}{\partial x_n} \\ \vdots & \ddots & \vdots \\ \frac{\partial y_m}{\partial x_1} & \cdots & \frac{\partial y_m}{\partial x_n} \end{bmatrix}_{x=x(t)} \tag{9}$$

where the number of state variables and measured outputs are denoted as n and m, respectively. There are different approaches to carry out the observability test. In this work, we use the Popov−Belevich−Hautus (PBH) rank test to check the observability of the WWTP.[13] The observability test is to check if the observability matrix O_k ($k = 1, ..., n$) has a full column rank:

$$\text{rank}(O_k) = n, \quad k = 1, ..., n \tag{10}$$

where

$$O_k = \begin{bmatrix} \lambda_k I - A \\ C \end{bmatrix}, \quad k = 1, ..., n \tag{11}$$

where n is the number of differential states, which is also the dimension of A. λ_k is the kth eigenvalue of A, and I is the identity matrix. If the linear approximation is observable at all the selected points along the typical state trajectories, the nonlinear system is also observable in neighborhoods of the typical trajectories.

In a distributed framework, the subsystem observability should be checked before performing distributed state estimation. For subsystem i, its observability is checked based on the pair (A_{ii}, C_i), which are the corresponding blocks in A and C to subsystem i.

Using the above approach, we first test the observability of the five biological rectors and the ideal splitter based on different sets of measurements. It is found that the entire states of each of the biological reactors can be observed based on a few of the measurable states of the same reactor. However, the splitter is not observable based only on the measurable states of the splitter itself. It is also found that the states of the splitter are observable based on a combination of certain measurable states of the splitter itself and the measurable states of reactor 1. To achieve a balance in terms of number of states, the entire WWTP is decomposed into two subsystems.

(1) Subsystem 1: Ideal splitter and Anoxic compartments (reactor 1 and reactor 2);
(2) Subsystem 2: Aerated compartments (reactor 3, reactor 4, and reactor 5).

Each subsystem model contains 39 state variables and 24 measurable states. The balanced number of state variables in the two subsystems makes the decomposition more favorable than others from a computational and communicational points of view. Once the subsystem decomposition is determined, observability tests are performed for each subsystems based on different combinations of the measurable states to determine a minimum set of measurements that ensures observability of the subsystem. The minimum sets of measurements for the two subsystem are found to be

(1) Subsystem 1
- ideal splitter: COD_6, $S_{ALK,6}$
- reactor 2: COD_2, $COD_{f,2}$, TSS_2, $S_{O,2}$, $S_{ALK,2}$

(2) Subsystem 2
- reactor 3: COD_3, $COD_{f,3}$, TSS_3, $S_{ALK,3}$.

We should also check the observability of the entire system again based on the measurable states of the two subsystems. The entire system is verified to be observable with measurements given above. Note that the above minimum sets of measurements ensure the observability of the subsystems and the entire system. However, to have robust performance in the distributed state estimation design in the presence of process disturbances and measurement noise, it is recommended that some easy-to-measure measurements can be added to the minimum sets to increase the robustness of the estimation method.[13] In this work, the nitrate and ammonia measurements in the effluent ($S_{NO,6}$, $S_{NH,6}$) are added into subsystem 1; the measurements of oxygen in the aerated reactors (SO_3, SO_4, and SO_5) are added into subsystem 2.

Remark 1 In this work, we considered two subsystems in the decomposition of the entire wastewater treatment process. However, the subsystem decomposition approach can be applied in a straightforward fashion to decompose the process into more than two subsystems. In the decomposition, one requirement is that every subsystem is observable. In the WWTP, it is found that the states of each of the five biological reactors can be observed based on their own measurable states; however, the states of the splitter cannot be observed based on its own measurable states and must be combined with reactor 1 to guarantee its observability. When the entire plant is decomposed into subsystems, the above observation must be taken into account.

Remark 2 It is possible that the observability of the process may be checked using nonlinear approaches directly. Nonlinear approaches are normally based on Lie derivatives of the outputs. However, it could be very challenging in the evaluation of Lie derivatives for large-scale systems like the WWTP because high-order Lie derivatives are involved. The proposed approach is a more practical approach for checking the observability of a large-scale nonlinear system.

DISTRIBUTED EKF DESIGN

Design of Subsystem Filters. In this work, the distributed extended Kalman filters are designed. We denote the vectors of the state variables of the two subsystems as x_1 and x_2 and denote the vectors of measured outputs as y_1 and y_2, respectively. The two subsystems can be described as the following forms:

$$\dot{x}_1(t) = f_1(x_1(t), x_2(t), u(t), w_1(t)) \tag{12a}$$
$$y_1(t) = C_1x_1(t) + v_1(t) \tag{12b}$$
$$\dot{x}_2(t) = f_2(x_1(t), x_2(t), u(t), w_2(t)) \tag{12c}$$

DOI: 10.1021/acs.iecr.6b00529
Ind. Eng. Chem. Res. 2016, 55, 7720−7729

$$y_2(t) = C_2 x_2(t) + v_2(t) \tag{12d}$$

where w_1 and w_2 are the process noise and v_1 and v_2 are the measurement noise in their respective subsystems. Note that the two subsystems are coupled via their states.

Extended Kalman filters are discrete time filters for nonlinear systems based on successive linearization of the nonlinear system. EKF consists of a prediciton step and an update step. Past data are processed and propagated by means of suitable statistics. In the design of distributed EKF for WWTP, each subsystem is associated with a local EKF which is evaluated at every sampling time t_k; the EKF associated with subsystem i (i = 1, 2) will be referred to as EKF i, and it is designed as follows:

(1) Prediction step:

$$\hat{x}_i(t_k|t_{k-1}) = \hat{x}_i(t_{k-1}) + \int_{t_{k-1}}^{t_k} f_i(\hat{x}_1(t), \hat{x}_2(t), u(t), 0)\,dt \tag{13a}$$

$$P_i(t_k|t_{k-1}) = A_i(t_{k-1})P_i(t_{k-1})A_i(t_{k-1})^T + Q_i \tag{13b}$$

(2) Update step:

$$K_i(t_k) = P_i(t_k|t_{k-1})C_i^T(C_iP_i(t_k|t_{k-1})C_i^T + R_i)^{-1} \tag{14a}$$

$$\hat{x}_i(t_k) = \hat{x}_i(t_k|t_{k-1}) + K_i(t_k)(y_i(t_k) - C_i\hat{x}_i(t_k|t_{k-1})) \tag{14b}$$

$$P_i(t_k) = (I - K_i(t_k)C_i)P_i(t_k|t_{k-1}) \tag{14c}$$

where eqs 13a and 13b are prediction steps and eqs 14a−14c are update steps. $\hat{x}_i(t_k|t_{k-1})$ denotes the prediction of the state at time instant t_k based on the state estimate $\hat{x}_i(t_{k-1})$ at t_{k-1} and subsystem model f_i. $P_i(t_{k-1})$ describes the error convariance matrix of $\hat{x}_i(t_{k-1})$, and $P_i(t_k|t_{k-1})$ predicts the error convariance matrix at time t_k based on the corresponding value at t_{k-1}. The matrices Q_i and R_i denote the convariances of process noise and measurement of subsystem i, respectively. $A_i(t_{k-1})$ is the Jacobian of f_i with respect to x_i at time t_{k-1}, and $K_i(t_k)$ is the filter gain at t_k. Based on eq 13a, it can be seen that EKF i needs information on both subsystem states (i.e., x_1 and x_2). This implies that the two distributed EKFs need to communicate to exchange their state estimates. The distributed estimation algorithm in the following section describes the detailed implementation of the distributed EKFs.

Remark 3 Note that a better computational efficiency may be achieved via further decomposition of the entire process into more subsystems. Parallel computation is also a feasible solution to have improved computational efficiency.[19]

Distributed State Estimation Algorithm. In this section, we discuss the detailed distributed state estimation algorithm which specifies how the two distributed EKFs should work collaboratively. We assumed that each local EKF has immediate access to the output measurements of its associated subsystem and it can also communicate with the other subsystem to exchange their subsystem state estimates. The exchanged information is used to compensate for the interacitons between the two subsystems in order to improve their state estimates.

The proposed distributed EKF scheme uses the following algorithm to carry out the state estimation of the WWTP:

Algorithm 1 Distributed extended Kalman filter algorithm

1. At t_0 = 0, the two EKFs are initialized with the initial subsystem state guesses $\hat{x}_i(0)$, i = 1, 2, and the subsystem output measurements $y_i(0)$, i = 1, 2.

2. At $t_k > 0$, carry out the following steps:

2.1 EKF i receives the output measurement $y_i(t_k)$, i = 1, 2.

2.2 Each EKF receives the subsystem state estimates of the previous time instant from the other subsystem; that is, EKF i, i = 1, 2, receives $\hat{x}_j(t_{k-1})$, j = 1, 2, $j \neq i$.

2.3 On the basis of both the local measurement and information from other subsystems, each EKF calculates the estimate of its subsystem's state; that is, EKF i calculates $\hat{x}_i(t_k)$, i = 1, 2. The estimate of the entire system state is $\hat{x}(t_k) = [\hat{x}_1(t_k)^T\ \hat{x}_2(t_k)^T]^T$.

2.4 EKF i sends the current information (i.e., $\hat{x}_i(t_k)$, i = 1, 2) to the other subsystems.

3. Go to step 2 at the next sampling time t_{k+1}.

Note that the process input information (i.e., $u(t)$) is assumed to be known to both of the EKFs. Note also that in the prediction step of EKF i at t_k, $\hat{x}_j(t_{k-1})$ is used to approximate $x_j(t)$ for $t \in [t_{k-1}, t_k)$ in eq 13a.

SIMULATIONS

In this section, we apply the distributed EKF scheme described above to the WWTP and compare its estimation performance with a centralized EKF under different weather conditions.

Simulation Settings. The performance of the distributed EKF and the centralized EKF will be compared under three different weather conditions: dry, rain, and storm. The data files of different weather conditions can be found on the International Water Association website.[20] The file of dry conditions contains two same weeks of dynamic dry weather influent data; the file of rain conditions contains 1 week of dynamic dry conditions influent data and a long rain event during the second week; the file of storm conditions contains 1 week of dynamic dry conditions data and two storm events superimposed on the dry conditions data during the second week. The initial conditions in the simulations for the biological reactor and the ideal splitter are shown in Table 5. These initial values are calculated by simulating the plant for a period of 100 days with constant inputs (average dry conditions flow rate, flow-weighted average influent concentrations) followed by a period of 14 days under dry conditions. The model parameters used in this work are shown in Table 4. Because the data of the first week under the three different weather conditions are all the same dry conditions influent data, we do the simulations only for the second week with the initial conditions shown in Table 5.

Table 4. Model Parameters

volume of compartment 1 (V_1)	1000 m^3
volume of compartment 2 (V_2)	1000 m^3
volume of compartment 3 (V_3)	1333 m^3
volume of compartment 4 (V_4)	1333 m^3
volume of compartment 5 (V_5)	1333 m^3
volume of splitter (V_6)	250 m^3
wastage flow rate (Q_w)	385 m^3/d
return sludge flow rate (Q_r)	18 846 m^3/d
internal recycle flow rate (Q_a)	55 338 m^3/d
oxygen transfer coefficient of compartment 3 (K_La_3)	240 l/d
Oxygen transfer coefficient of compartment 4 (K_La_4)	240 l/d
oxygen transfer coefficient of compartment 5 (K_La_5)	84 l/d

In the simulations, it is assumed that the entire process measurements are sampled synchronously and periodically at time instants $t_k \geq 0$ such that $t_k = t_0 + k\Delta$ where t_0 = 0 is the initial time, Δ = 15 min the sampling time interval, and k is a

DOI: 10.1021/acs.iecr.6b00529
Ind. Eng. Chem. Res. 2016, 55, 7720−7729

Table 5. Initial Conditions of the Biological Reactors (Units 1−5) and the Splitter (Unit 6)

unit i	1	2	3	4	5	6	unit
$S_{I,i}$	30	30	30	30	30	30	gCOD/m^3
$S_{S,i}$	2.69	1.41	1.22	0.97	0.86	0.86	gCOD/m^3
$X_{I,i}$	1219.35	1218.08	1215.74	1214.62	1214.73	2399.50	gCOD/m^3
$X_{S,i}$	80.83	75.09	63.68	54.52	48.17	94.17	gCOD/m^3
$X_{B,H,i}$	2586.76	2585.16	2583.14	2582.09	2581.71	5098.94	gCOD/m^3
$X_{B,A,i}$	150.77	150.47	150.76	151.19	151.45	299.09	gCOD/m^3
$X_{P,i}$	520.80	520.82	520.63	521.05	522.03	1031.23	gCOD/m^3
$S_{O,i}$	0.003872	0.00005674	1.68	2.32	0.44	0.44	g(−COD)/m^3
$S_{NO,i}$	6.09	4.33	7.26	10.15	11.32	11.35	gN/m^3
$S_{NH,i}$	8.19	8.81	6.14	3.49	2.16	2.12	gN/m^3
$S_{ND,i}$	1.18	0.87	0.81	0.75	0.67	0.66	gN/m^3
$X_{ND,i}$	5.16	4.91	4.29	3.79	3.44	6.74	gN/m^3
$S_{ALK,i}$	4.88	5.05	4.64	4.24	4.06	4.06	mol/m^3

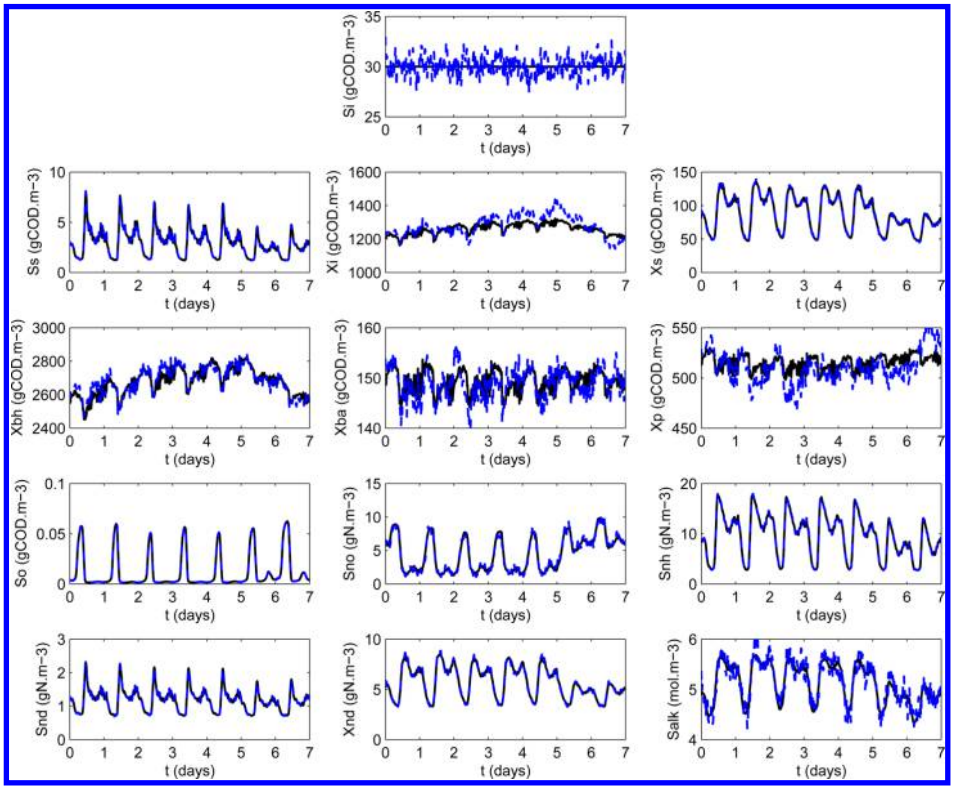

Figure 2. Trajectories of the actual process state (solid lines) and the estimates given by the EKF (dashed lines) of reactor 1 under dry conditions.

positive integer. In every set of simulations, the same process disturbance and measurement noise sequences and initial conditions are used in both the centralized EKF and the distributed EKF schemes. Process disturbances are considered as random and bounded. It is also assumed that the measured outputs are subject to bounded measurement noise.

Results of Dry Conditions. In this subsection, we compare the performance of the centralized EKF and the distributed EKF schemes under dry weather conditions. In the first set of simulations, the random process disturbances in the dynamics of the 78 states are generated with the zero mean, standard deviation vector being $0.2x_0$ and bounded between $-0.2x_0$ and $0.2x_0$; the bounded noise in the measurements is generated as normally distributed values with zero mean and standard deviation $0.2y_0$; the values are restricted to be in the interval $[-0.2y_0, 0.2y_0]$. The symbol x_0 denotes the initial conditions as shown in Table 5 and y_0 can be calculated by $y_0 = Cx_0$. The initial guess in the different estimation schemes is set to be $1.1x_0$. The parameters used in the EKF are $Q = \mathrm{diag}((0.2x_0)^2)$, $R = \mathrm{diag}((0.2y_0)^2)$, and $P(0) = Q = \mathrm{diag}((0.2x_0)^2)$ where the notation $\mathrm{diag}(v)$ represents a diagonal matrix whose diagonal elements are the elements of a vector v. The assumption that Q, R, and $P(0)$ are diagonal matrices means that the process noise, measurement noise, and state estimation errors are all uncorrelated. For the distributed EKF, the parameters of the two subsystems are set to be the same magnitude as in the centralized EKF; they are $Q_i = \mathrm{diag}((0.2x_{0,i})^2)$, $R_i = \mathrm{diag}((0.2y_{0,i})^2)$, and $P_i(0) = Q_i = \mathrm{diag}((0.2x_{0,i})^2)$, where $x_{0,i}$ and $y_{0,i}$ are the corresponding portion in x_0 and y_0 to subsystem i, $i = 1, 2$.

Figure 2 shows the actual state trajectories and the estimates of reactor 1 given by the centralized EKF. Figure 3 shows the actual state trajectories and the estimates of reactor 1 obtained using the distributed EKF. From the figures, it can be seen that both the EKF and the proposed distributed EKF can track the

DOI: 10.1021/acs.iecr.6b00529
Ind. Eng. Chem. Res. 2016, 55, 7720−7729

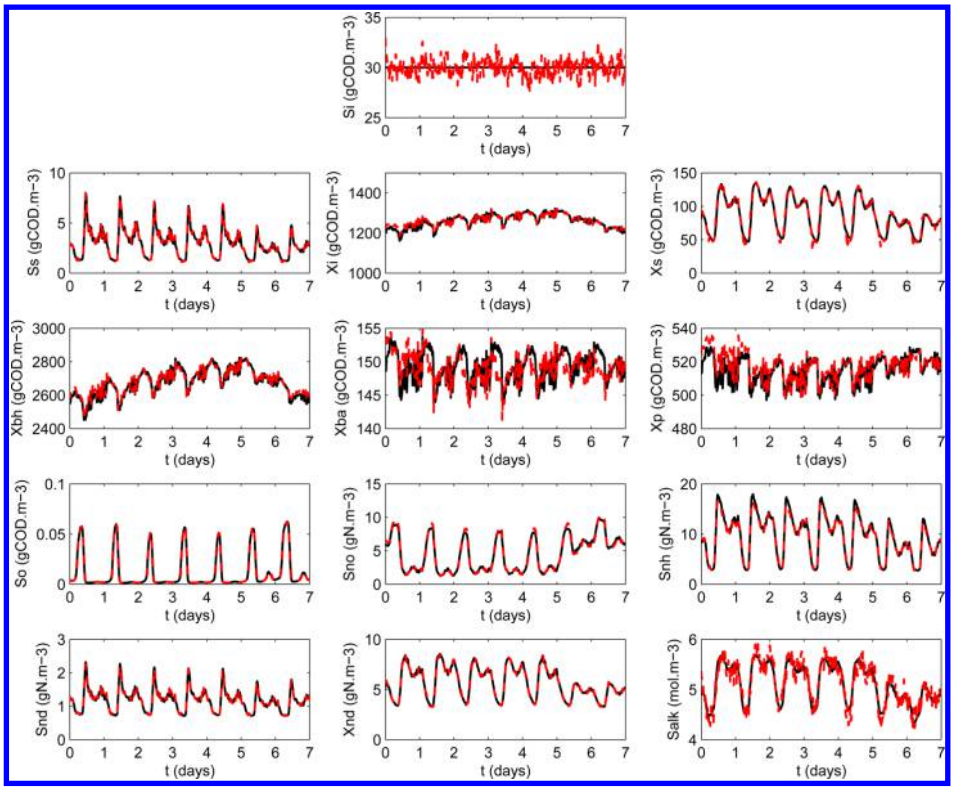

Figure 3. Trajectories of the actual process state (solid lines) and the estimates given by the distributed EKF (dashed lines) of reactor 1 under dry conditions.

trend of the actual system states well. To compare the performance of the EKF and the distributed EKF, we calculate the errors given by the two schemes. To account for the different magnitudes of the estimation errors for different states, the error for each state is normalized based on its maximum estimation error from the two estimation schemes. The Euclidean norms of the normalized estimation error is defined as

$$e(t_k) = \sqrt{\sum_{i=1}^{78} (e_i(t_k))^2} \tag{15}$$

where $e(t_k)$ is the normalized error of 78 states at time instant t_k and $e_i(t_k)$ is the normalized error of state i, i = 1, 2, ..., 78, defined as

$$e_i(t_k) = \frac{\hat{x}_i(t_k) - x_i(t_k)}{\max(\hat{x}_i - x_i)} \tag{16}$$

where the maximum error for a given state i is the largest error for state i among the EKF and the distributed EKF methods. It means that the error for each state is normalized based on its maximum estimation errors given by the two different schemes.

The mean values of the normalized estimation error can be defined as:

$$\text{Mean}|e| = \frac{1}{K}\sum_{k=1}^{K} e(t_k) \tag{17}$$

where K is the total number of samples over the simulation period. According to eqs 15−17, the mean values of the estimation errors over the 7 days given by the EKF and the distributed EKF are 2.7214 and 2.4144, respectively. The maximum values of estimation errors calculated by the EKF and the distributed EKF are 4.9174 and 4.5590, respectively. In this particular simulation, with the distributed EKF, there are approximately 11% and 7% improvements with respect to the centralized EKF in terms of mean and maximum estimation error. Figure 4 shows the trajectories of the Euclidean norms of

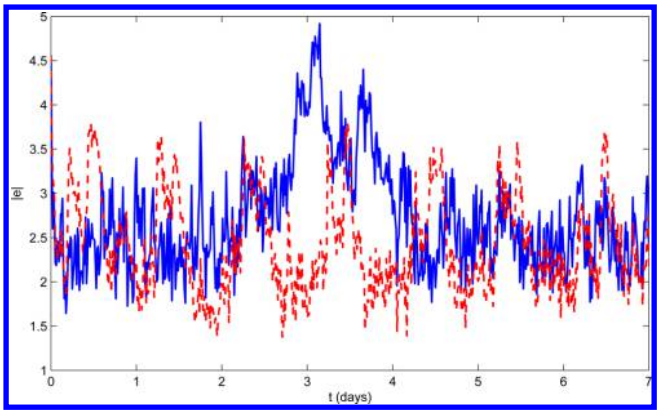

Figure 4. Trajectories of the Euclidean norm of normalized estimation errors given by the EKF (solid lines) and the distributed EKF (dashed lines) under dry conditions.

the normalized estimation errors given by the two different schemes. We note that there is no guarantee that the centralized scheme should give a better performance than the distributed scheme when EKF is applied to a nonlinear process.

In another set of simulations, the effect of process disturbance and measurement noise on the performance of the centralized EKF and the distributed EKF is studied. In this set of simulations, the same initial guess $(1.1x_0)$ as in the first set of simulations is used but with different process disturbance and measurement noise. We suppose the process noise is Gaussian

DOI: 10.1021/acs.iecr.6b00529
Ind. Eng. Chem. Res. 2016, 55, 7720−7729

white noise generated with the zero mean, standard deviation $w_Q x_0$, and bounded between $-w_Q x_0$ and $w_Q x_0$; the parameter Q used in the centralized EKF is $Q = \mathrm{diag}((w_Q x_0)^2)$. In the distributed EKF, Q_i is set to be $Q_i = \mathrm{diag}((w_Q x_{0,i})^2)$, $i = 1, 2$. The measurement noise is generated with zero mean, standard deviation being $w_R y_0$ and bounded between $-w_R y_0$ and $w_R y_0$; the corresponding parameters R used in the centralized EKF is $R = \mathrm{diag}((w_R y_0)^2)$, and $P(0)$ is set to be the same as Q. In the distributed EKF, $R_i = \mathrm{diag}((w_R y_{0,i})^2)$ and $P_i(0) = Q_i = \mathrm{diag}((w_Q x_{0,i})^2)$. The mean and maximum of the norm of the normalized estimation errors given by the EKF and the distributed EKF with different process noise and measurement noise are shown in Table 6. From the set of simulations, it can

Table 6. Performance Comparison for Different Schemes under Dry Conditions

	w_R	w_Q	centralized EKF	distributed EKF
Mean|e|	0.2	0.2	2.7214	2.4144
	0.1	0.1	2.4058	2.4032
	0.05	0.05	1.8391	2.2911
	0.2	0.1	2.2831	2.2493
	0.1	0.2	2.7224	2.7134
	0.2	0.05	1.8339	2.6252
	0.05	0.2	2.6746	2.7615
Max|e|	0.2	0.2	4.9174	4.5590
	0.1	0.1	5.7256	5.7256
	0.05	0.05	6.3614	6.3614
	0.2	0.1	6.0740	6.0740
	0.1	0.2	4.9115	4.9115
	0.2	0.05	7.4000	7.4000
	0.05	0.2	4.9379	5.0508
CPU time			1.82 s	1.03 s

be seen that the centralized EKF is much more sensitive to the properties of the noise sequences. With different noise sequences, the centralized EKF gives quite different performance. The overall trend is that the performance of the centralized EKF decreases obviously with the increase of the magnitude of the noise. However, the distributed EKF has a rather stable performance in terms of mean error under these different noise realizations. When the noise is small, the centralized EKF overall gives better performance; when the noise is increased, the distributed EKF may give better performance. Note that the two schemes have similar performance in terms of the maximum error.

From the simulations, we found that the distributed EKF has a rather stable performance in terms of mean error under different noise realizations. One possible explanation is that in the distributed framework, the noise of a subsystem is restricted to be within the subsystem and is essentially isolated from the other subsystem. While in the centralized framework, the noise of one subsystem is propagated into the other subsystem via the centralized model. This also implies that the distributed EKF has the potential to give a better performance in terms of fault tolerance. The average CPU times used in the evaluation of the estimation methods at one sampling time are also compared and shown in Table 6. It can be seen that the evaluation time of the distributed EKF is significantly (43%) less than that of the centralized EKF. Note that all the simulations are carried out in MATLAB using an Intel Core i5 computer at 1.80 GHz with 4GB RAM.

Results of Rain and Storm Conditions. In this section, the estimation performance given by the proposed distributed EKF and the centralized EKF are compared under rain and storm conditions. We also assume that the process noise and measurement noise are random Gaussian white noise with zero mean, standard deviation $w_Q x_0$ and $w_R y_0$, respectively. The initial guess in both schemes is set to be $1.1x_0$. The parameters Q and R used in the centralized EKF are $Q = \mathrm{diag}((w_Q x_0)^2)$ and $R = \mathrm{diag}((w_R y_0)^2)$, respectively. $P(0)$ is set to be the same as Q. In the distributed EKF, the corresponding parameters are set as $Q_i = \mathrm{diag}((w_Q x_{0,i})^2)$, $R_i = \mathrm{diag}((w_R y_{0,i})^2)$, and $P_i(0) = Q_i = \mathrm{diag}((w_Q x_{0,i})^2)$.

In the first set of simulations, the w_Q and w_R are both set to be 0.2. Figures 5 and 6 show the actual state trajectories and the

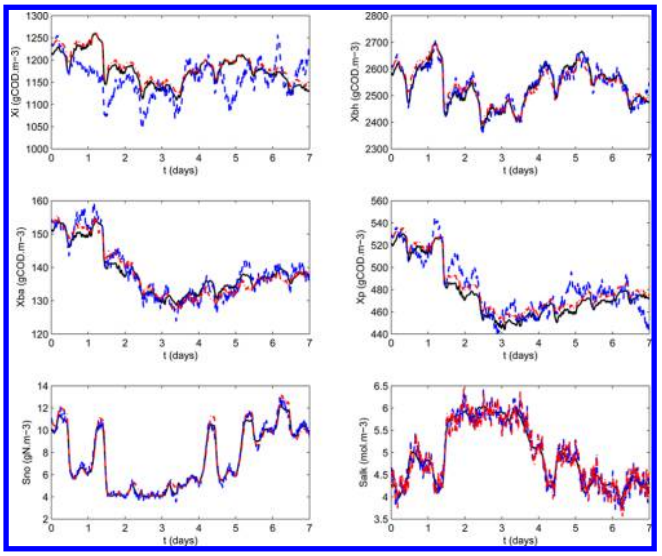

Figure 5. Trajectories of the actual process state (solid lines) and the estimates given by the EKF (dashed lines) and the distributed EKF (dash-dotted lines) of reactor 4 under rain conditions.

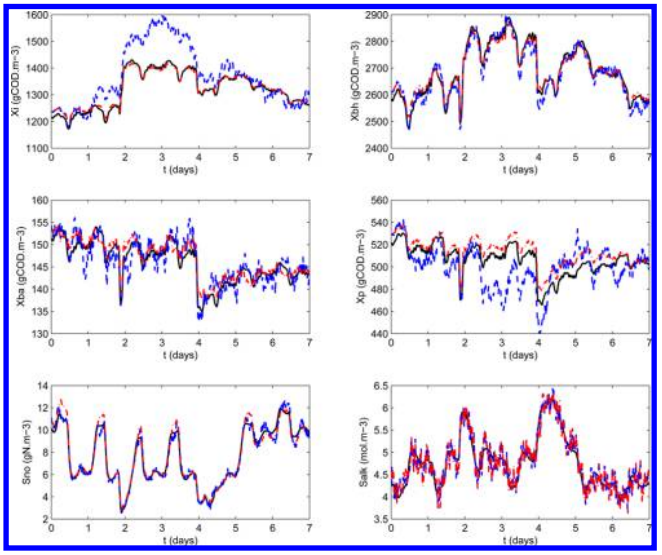

Figure 6. Trajectories of the actual process state (solid lines) and the estimates given by the EKF (dashed lines) and the distributed EKF (dash-dotted lines) of reactor 4 under storm conditions.

estimates given by the distributed EKF and the centralized EKF of reactor 4 under rain and storm conditions, respectively. Note that only 6 concentrations of the total 13 states of reactor 4 are shown in the figures for brevity. Note also that the estimates

DOI: 10.1021/acs.iecr.6b00529
Ind. Eng. Chem. Res. 2016, 55, 7720−7729

and states in other reactors and the splitter have similar patterns. Under the rain conditions, the mean values of estimation errors calculated by the distributed EKF and the centralized EKF are 2.4870 and 2.5673, respectively. With respect to the centralized EKF, the distributed EKF gives 3.1% improvement. On the other hand, under the storm conditions, the mean values of estimation errors given by the distributed EKF and the centralized EKF are 2.3717 and 2.5651, respectively. In this set of simulations, with the distributed EKF, there is 7.5% improvement with respect to the centralized EKF.

In another set of simulations, the magnitude of w_Q and w_R are adjusted to study the effect of process disturbance and measurement noise on estimation performance under rain and storm conditions. The results are shown in Tables 7 and 8.

Table 7. Performance Comparison for Different Schemes under Rain Conditions

	w_R	w_Q	centralized EKF	distributed EKF
Meanlel	0.2	0.2	2.5673	2.4870
	0.1	0.1	1.4807	1.7885
	0.05	0.05	0.7550	1.5163
Maxlel	0.2	0.2	4.3318	4.5478
	0.1	0.1	4.3318	4.3318
	0.05	0.05	4.3318	4.3318
CPU time			1.91 s	1.13 s

Table 8. Performance Comparison for Different Schemes under Storm Conditions

	w_R	w_Q	centralized EKF	distributed EKF
Meanlel	0.2	0.2	2.5651	2.3717
	0.1	0.1	1.2175	1.6266
	0.05	0.05	0.7091	1.3988
Maxlel	0.2	0.2	4.0139	4.1396
	0.1	0.1	3.9355	3.9355
	0.05	0.05	3.9355	3.9355
CPU time			1.90 s	1.09 s

It can be seen that the obtained conclusions are similar to those under dry conditions. Note that because there are larger fluctuations on the process states under rain and storm conditions than under dry conditions, when the noise is greater under the rain and storm conditions, the distributed EKF may give better performance. In terms of average CPU times, it can be seen that the evaluation time of the distributed EKF is still significantly less than the centralized EKF.

CONCLUSIONS

In this work, we proposed a distributed EKF scheme and applied it to the wastewater treatment process and compared its estimation performance with a centralized EKF. A benchmark simulation model based on BSM1 was used to simulate the WWTP under different weather conditions. The simulation results demonstrated that the distributed EKF may improve the mean error by 3−11% compare to the centralized EKF under different weather conditions with larger disturbance noise and measurement noise. The results also showed the distributed EKF has a rather more stable performance than the centralized EKF in terms of mean error under different noise realizations, which implies the distributed EKF has the potential to give a better performance in terms of fault tolerance. In addition, the evaluation time of the distributed EKF is significantly less than that of the centralized EKF.

AUTHOR INFORMATION

Corresponding Author

*E-mail: jinfeng@ualberta.ca.

Funding

Financial support from the National Natural Science Foundation of China (61503257 and 61374112); the Natural Science Foundation of Liaoning Province, China (2014020138); the Program for Liaoning Province Distinguished Young Scholars in University (LJQ2014045); and the University of Alberta (RES0014908) is acknowledged.

Notes

The authors declare no competing financial interest.

REFERENCES

(1) Machado, V. C.; Gabriel, D.; Lafuente, J.; Baeza, J. A. Cost and effluent quality controller design based on the relative gain array for a nutrient removal WWTP. *Water Res.* **2009**, *43*, 5129−5141.

(2) de Araujo, A. C. B.; Gallani, S.; Mulas, M.; Olsson, G. Systematic approach to the design of operation and control policies in activated sludge systems. *Ind. Eng. Chem. Res.* **2011**, *54*, 8542−8557.

(3) Vrecko, D.; Hvala, N.; Stare, A.; Burica, O.; Strazar, M.; Levstek, M.; Cerar, P.; Podbevsek, S. Improvement of ammonia removal in activated sludge process with feedforward-feedback aeration controllers. *Water Sci. Technol.* **2006**, *53*, 125−132.

(4) Mayne, D. Q.; Rawlings, J. B.; Rao, C. V.; Scokaert, P. O. M. Constrained model predictive control: Stability and optimality. *Automatica* **2000**, *36*, 789−814.

(5) O'Brien, M.; Mack, J.; Lennox, B.; Lovett, D.; Wall, A. Model predictive control of an activated sludage process: A case study. *Control Engineering Practice* **2011**, *19*, 54−61.

(6) Francisco, M.; Vega, P.; Revollar, S. Model predictive control of BSM1 benchmark of wastewater treatment process: A tuning procedure. *50th IEEE Conference on Decision and Control and European Control Conference*, Orlando, FL, 2011.

(7) Han, H. G.; Qiao, J. F. Nonlinear model-predictive control for industrial processes: an application to wastewater treatment process. *IEEE Transactions on Industrial Electronics* **2014**, *61*, 1970−1982.

(8) Vega, P.; Revollar, S.; Francisco, M.; Martin, J. M. Integration of set point optimization techniques into nonlinear MPC for improving the opration of WWTPs. *Comput. Chem. Eng.* **2014**, *68*, 78−95.

(9) Duzinkiewicz, K.; Brdys, M. A.; Kurek, W.; Piotrowski, R. Genetic hybrid predictive controller for optimized dissolved-oxygen tracking at lower control level. *IEEE Transactions on Control Systems Technology* **2009**, *17*, 1183−1190.

(10) Zeng, J.; Liu, J. Economic model predictive control of wastewater treatment processes. *Ind. Eng. Chem. Res.* **2015**, *54*, 5710−5721.

(11) Einicke, G. A. *Smoothing, Filtering and Prediction: Estimating the Past, Present and Future*; Intech: Croatia, 2012.

(12) Robertson, D. G.; Lee, J. H.; Rawlings, J. B. A moving horizon-based approach for least-squares estimation. *AIChE J.* **1996**, *42*, 2209−2224.

(13) Busch, J.; Elixmann, D.; Kuhl, P.; Gerkens, C.; Schloder, J. P.; Bock, H. G.; Marquardt, W. State estimation for large-scale wastewater treatment plants. *Water Res.* **2013**, *47*, 4774−4787.

(14) Christofides, P. D.; Scattolini, R.; Muñoz de la Peña, D.; Liu, J. Distributed model predictive control: A tutorial review and future research directions. *Comput. Chem. Eng.* **2013**, *51*, 21−41.

(15) Zhang, J.; Liu, J. Distributed moving horizon estimation for nonlinear systems with bounded uncertainties. *J. Process Control* **2013**, *23*, 1281−1295.

(16) Zeng, J.; Liu, J. Distributed moving horizon state estimation: Simultaneously handling communication delays and data losses. *Systems & Control Letters* **2015**, *75*, 56−68.

(17) Alex, J.; Benedetti, L.; Copp, J.; Gernaey, K. V.; Jeppsson, U.; Nopens, I.; Pons, M. N.; Rieger, L.; Rosen, C.; Steyer, J. P.; Vanrolleghem, P.; Winkler, S. Benchmark Simulation Model No. 1

DOI: 10.1021/acs.iecr.6b00529
Ind. Eng. Chem. Res. 2016, 55, 7720−7729

(BSM1). Technical Report; Department of Industrial Electrical Engineering and Automation, Lund University: Lund, Sweden, 2008.
(18) Chen, C. *Linear System Theory and Design*, 4th ed.; Oxford University Press: New York, 2012.
(19) Kwon, J. S. I.; Nayhouse, M.; Christofides, P. D. Multiscale, multidomain modeling and parallel computation: Application to crystal shape prediction in crystallization. *Ind. Eng. Chem. Res.* **2015**, *54*, 11903−11914.
(20) International Water Association. http://www.benchmarkwwtp.org.

DOI: 10.1021/acs.iecr.6b00529
Ind. Eng. Chem. Res. 2016, 55, 7720−7729